# Orbits in a stochastic Schwarzschild geometry

Roberto Casadio,[1,2,*] Andrea Giusti,[3,†] and Andrea Mentrelli[4,‡]

[1] *Dipartimento di Fisica e Astronomia, Alma Mater Università di Bologna, via Irnerio 46, 40126 Bologna, Italy*
[2] *I.N.F.N., Sezione di Bologna, IS FLAG viale B. Pichat 6/2, I-40127 Bologna, Italy*
[3] *Department of Physics & Astronomy, Bishop's University, 2600 College Street, J1M 1Z7 Sherbrooke, Québec, Canada*
[4] *Alma Mater Research Center on Applied Mathematics ($AM^2$), Dipartimento di Matematica, Università di Bologna, Via Saragozza 8, I-40123 Bologna, Italy*

We study geodesics in the Schwarzschild space-time affected by an uncertainty in the mass parameter described by a Gaussian distribution. This study could serve as a first attempt at investigating possible quantum effects of black hole space-times on the motion of matter in their surroundings as well as the role of uncertainties in the measurement of the black hole parameters.

arXiv:1901.06206v2 [gr-qc] 18 Jul 2019

* casadio@bo.infn.it
† agiusti@bo.infn.it
‡ andrea.mentrelli@unibo.it

## I. INTRODUCTION

Black holes were always one of the characterising predictions of General Relativity (GR) [1, 2], and the recent detection of gravitational waves from the merging of black hole binaries [3] has further boosted the interest in such astrophysical objects. The mathematical properties of these vacuum solutions of the Einstein equations are already problematic at the classical level, where it is well known that no sensible energy-momentum tensor can be associated with them [4]. It becomes even more problematic at the quantum level, since our very limited understanding from semiclassical approaches yield the famous Hawking radiation [5] and a bunch of paradoxes (see, e.g. Refs. [6–11] and references therein).

On the other hand, our observational capacities remain relatively weak in determining with precision what astrophysical black holes are in nature, and a host of alternative, somewhat more exotic, compact objects are actively being investigated in the present literature (see e.g. Refs. [11–22]). In this respect, it is very important to determine the physical consequences of alternative models of compact objects or alternative descriptions of gravity on observable quantities, regardless of the origin of such deviations from the simple black hole metrics of GR.

For example, the Horizon Quantum Mechanics [23–26] offers an alternative perspective to the semiclassical approach to gravity, whose aim is to put under the spotlight the quantum features of a black hole's geometric structure inherited by a purely quantum mechanical description of its source. In this regard, the location of trapping surfaces becomes fuzzy because of the quantum mechanical nature of the source, thus providing a clear motivation for the study presented here.

Another motivation can be found in light of the theory of stochastic gravity (see e.g. [27] and references therein), which offers an extension of semiclassical gravity based on the classical Einstein equations sourced by the stress-energy tensor of quantum matter fields by including the contribution of quantum fluctuations to the vacuum expectation values of matter. Specifically, these fluctuations are accounted for by means of a noise kernel bitensor, and the semiclassical Einstein equations are replaced by the so called Einstein-Langevin equations.

In this work, after reviewing some generalities on the structure of the orbits in both Newtonian gravity and GR, we analyze the geodesics of a Schwarzschild space-time [1] [28, 29]

$$\mathrm{d}s^2 = -\left(1-\frac{2\,G\,M}{r}\right)\mathrm{d}t^2 + \left(1-\frac{2\,G\,M}{r}\right)^{-1}\mathrm{d}r^2 + r^2\left(\mathrm{d}\theta^2+\sin^2\theta\,\mathrm{d}\varphi^2\right)\ , \tag{1}$$

affected by an uncertainty in the mass parameter modeled in terms of a Gaussian distribution.

## II. ORBITS IN NEWTONIAN GRAVITY AND IN THE SCHWARZSCHILD GEOMETRY

The equation that governs the radial motion of a test particle in the Schwarzschild metric (1) or in Newtonian physics can be written as [1, 2]

$$\frac{1}{2}\left(\frac{\mathrm{d}r}{\mathrm{d}\tau}\right)^2 = \frac{E^2}{2} - V(r) \equiv \mathcal{E} - V(r)\ , \tag{2}$$

where we denoted with $E$ and $L$, respectively, the conserved energy and angular momentum per unit mass in the massive case ($\varepsilon = 1$), or the conserved energy and angular momentum in the massless case ($\varepsilon = 0$). The potential in the above equation reads

$$V(r) = \frac{\varepsilon}{2}\left(1-\frac{2\,G\,M}{r}\right) + \frac{L^2}{2\,r^2} - \gamma\,\frac{G\,M\,L^2}{r^3}\ , \tag{3}$$

where the parameter $\gamma = 1$ in GR and $\gamma = 0$ (and $\varepsilon = 1$) in Newtonian gravity. Eq. (2) formally resembles the equation for a classical particle of unit mass and energy $\mathcal{E}$ moving in a one-dimensional potential [2] $V$ (the conserved energy per unit mass is $E$, but the effective potential corresponds to $\mathcal{E} = E^2/2$).

---

[1] We use units with $c = 1$ and denote the Newton constant with $G$.

[2] The potential $V$ is actually the *potential energy* (per unit mass).

### A. Circular orbits

The stationary points of the potential $V$ represent circular orbits, whose radius $r_{\rm c}$ is thus given by

$$0 = \left.\frac{dV}{dr}\right|_{r=r_{\rm c}} \sim \varepsilon\, G\, M\, r_{\rm c}^2 - L^2\, r_{\rm c} + 3\,\gamma\, G\, M\, L^2 \ . \tag{4}$$

Of course, these circular orbits are stable (unstable) if they correspond to a minimum (maximum) of the potential.

#### *1. Newtonian gravity*

In Newtonian gravity ($\gamma = 0$), we have the following well-known results:

a) For massless particles ($\varepsilon = 0$) no circular orbits exist. In fact, bound orbits do not exist in general (massless particles move on a straight line).

b) For massive particles ($\varepsilon = 1$) there are stable circular orbits at the radius

$$r_{\rm c} = \frac{L^2}{G\, M} \ , \tag{5}$$

as well as bound orbits that oscillate around the radius $r_{\rm c}$. In general, if the energy is greater than the asymptotic value [3] $E = 1$, the orbits are unbound (parabolas or hyperbolas), otherwise they are bound (circles or ellipses).

#### *2. General Relativity*

In GR ($\gamma = 1$), the term $G\, M\, L^2/r^3$ becomes important when $r$ is small and the potential $V$ vanishes at the Schwarzschild radius $r = 2\, G\, M$. The following general results are also well-known:

a) For massless particles ($\varepsilon = 0$), we find

$$r_{\rm c} = 3\, G\, M \equiv r_{\rm ph} \ , \tag{6}$$

which represents the innermost (unstable) circular orbit of a photon. Note that the radius of this orbit does not depend on $L$.

b) For massive particles ($\varepsilon = 1$), the zeros of Eq. (4) are given by

$$r_\pm = \frac{L^2}{2\, G\, M}\left(1 \pm \sqrt{1 - \frac{12\, G^2\, M^2}{L^2}}\right) \equiv \frac{L^2\,(1 \pm \chi)}{2\, G\, M} \ . \tag{7}$$

Hence, when $L > \sqrt{12}\, G\, M \approx 3.46\, GM$ (that is $\chi$ is real), there is an inner unstable circular orbit ($r_{\rm in} = r_-$) and a outer stable circular orbit ($r_{\rm out} = r_+$). For large $L$, we have

$$\lim_{L\to\infty} r_{\rm in} = 3\, G\, M \ , \tag{8}$$

so that the unstable orbit approaches the massless orbit (6), whereas

$$r_{\rm out} \sim \frac{L^2}{G\, M} \tag{9}$$

and the stable circular orbit moves farther and farther away, approaching the Newtonian expression (5). Conversely, decreasing $L$ the two orbits come closer together and coincide for $L = \sqrt{12}\, G\, M$. The common radius of this (stable) circular orbit is [4]

$$r_{\rm c} = 2\, r_{\rm ph} = 6\, G\, M \ . \tag{10}$$

Finally, no circular orbits are possible when $L < \sqrt{12}\, G\, M$ (since $\chi$ becomes imaginary).

---

[3] This follows from $V(r \to \infty) = 1/2$ in Eq. (2).

[4] This is the Innermost Stable Circular Orbit (ISCO).

### B. Non-circular orbits

Non-circular orbits in GR are not perfectly closed ellipses. Nonetheless, they can be viewed, to a good level of approximation, as ellipses that precess. Thus, it is rather convenient to describe the evolution of the radial coordinate $r$ as a function of the angular coordinate $\varphi$, i.e. $r = r(\varphi)$.

Recalling that $L = r^2\,\mathrm{d}\varphi/\mathrm{d}\tau$ [1], from Eq. (2) we obtain

$$\left(\frac{\mathrm{d}r}{\mathrm{d}\varphi}\right)^2 = \frac{E^2-\varepsilon}{L^2}\,r^4 + \frac{2\,\varepsilon\,G\,M}{L^2}\,r^3 - r^2 + 2\,\gamma\,G\,M\,r\ . \tag{11}$$

Letting $x \equiv L^2/G\,M\,r$, Eq. (11) becomes

$$\left(\frac{\mathrm{d}x}{\mathrm{d}\varphi}\right)^2 = \frac{L^2\left(E^2-\varepsilon\right)}{G^2\,M^2} + 2\,\varepsilon\,x - x^2 + \gamma\,\frac{2\,G^2\,M^2}{L^2}\,x^3\ , \tag{12}$$

which, upon differentiating with respect to $\varphi$, can also be written as

$$\frac{\mathrm{d}^2x}{\mathrm{d}\varphi^2} = \varepsilon - x + \gamma\,\frac{3\,G^2\,M^2}{L^2}\,x^2\ . \tag{13}$$

Note that $x = 1$ corresponds to the Newtonian circular orbit (5).

For the purpose of finding analytical solutions to Eq. (12), we define the dimensionless parameters

$$\alpha = \frac{G\,M}{L}\ , \qquad \beta = \frac{G\,M}{E\,L} = \frac{\alpha}{E}\ , \qquad \rho = \frac{2\,G^2\,M^2}{L^2} = 2\,\alpha^2\ , \tag{14}$$

so that Eq. (12) will read

$$\left(\frac{\mathrm{d}x}{\mathrm{d}\varphi}\right)^2 = \left(\frac{1}{\beta^2} - \frac{\varepsilon}{\alpha^2}\right) + 2\,\varepsilon\,x - x^2 + \gamma\,\rho\,x^3\ . \tag{15}$$

Analogously, Eq. (13) can be rewritten as

$$\frac{\mathrm{d}^2x}{\mathrm{d}\varphi^2} = \varepsilon - x + \frac{3}{2}\,\gamma\,\rho\,x^2\ . \tag{16}$$

#### 1. *Newtonian gravity*

For Newtonian gravity ($\gamma = 0$), Eq. (15) reduces to

$$\begin{aligned}\left(\frac{\mathrm{d}x}{\mathrm{d}\varphi}\right)^2 &= \left(\frac{1}{\beta^2} - \frac{\varepsilon}{\alpha^2}\right) + 2\,\varepsilon\,x - x^2 \\ &\equiv -\left(x - x_1\right)\left(x - x_2\right)\ ,\end{aligned} \tag{17}$$

where the roots $x_1 = \varepsilon - \kappa$ and $x_2 = \varepsilon + \kappa$, with

$$\kappa = \sqrt{\frac{1}{\beta^2} - \frac{\varepsilon}{\alpha^2} + \varepsilon^2}\ . \tag{18}$$

The general solution to Eq. (17) is then given by

$$\begin{aligned}x(\varphi) &= x_1 + (x_2 - x_1)\sin^2\left(\frac{\varphi}{2} + \delta\right) \\ &= \varepsilon + (x_1 - \varepsilon)\cos(\varphi + 2\,\delta)\,,\end{aligned} \tag{19}$$

where $\delta$ is an integration constant determined by the initial condition $x(\varphi_0) = x_0$. Eq. (19) describes a conic of eccentricity

$$e = \frac{x_2 - x_1}{x_2 + x_1} = \frac{\kappa}{\varepsilon}\ . \tag{20}$$

For massive particles ($\varepsilon = 1$), we see that:

- if $x_1 > 0$ and $x_1 \neq x_2$ (i.e. $0 < \kappa < 1$), the orbit is an ellipse where $x_1$ and $x_2$ represent the distances of furthest and closest approach, respectively;
- if $x_1 = x_2$ (i.e. $\kappa = 0$), the orbit is circular, with radius given by the Newtonian value (5) (this happens when $E^2 = 1 - G^2\, M^2/L^2$);
- if $x_1 = 0$ (i.e. $\kappa = 1$, namely $\alpha = \beta$), the orbit is a parabola and $x_2$ represents the distance of closest approach;
- if $x_1 < 0$ (i.e. $\kappa > 1$), the orbit is a hyperbola, and $x_2$ represents again the distance of closest approach.

For massless particles ($\varepsilon = 0$), $-\kappa \leq x \leq \kappa$ and the orbit is always an unbound straight line.

### *2. General Relativity*

In the GR case ($\gamma = 1$), the cubic polynomial on the right-hand side of Eq. (15) admits three roots, which we denote by $x_1$, $x_2$ and $x_3$, so that

$$\left(\frac{\mathrm{d}x}{\mathrm{d}\varphi}\right)^2 = \rho\,(x - x_1)\,(x - x_2)\,(x - x_3)\ , \tag{21}$$

with $x_1 + x_2 + x_3 = 1/\rho$. The general solution of Eq. (21) is

$$x\,(\varphi) = x_1 + (x_2 - x_1)\,\mathrm{sn}^2\left(\frac{\varphi}{2}\,\sqrt{\rho\,(x_3 - x_1)} + \delta,\, k\right)\ , \tag{22}$$

where $\mathrm{sn}\,(z,\, k)$ is the Jacobi elliptic function with argument $z$ and elliptic modulus

$$k = \sqrt{\frac{x_2 - x_1}{x_3 - x_1}}\ . \tag{23}$$

The integration constant $\delta$ is again found from the initial condition $x(\varphi_0) = x_0$.

The roots $x_1$, $x_2$ and $x_3$ can either be all real, or one real and two complex conjugates. In the first case, we name the roots such that $x_1 \leqslant x_2 \leqslant x_3$, while in the second case we denote the real root as $x_1$. The following situations are therefore possible:

- $\boldsymbol{x_1 < x_2 < x_3}$: if all three roots are distinct real numbers, the second derivative

$$\frac{\mathrm{d}^2 x}{\mathrm{d}\varphi^2} = \frac{\rho}{2}\,[(x - x_2)\,(x - x_3) + (x - x_1)\,(x - x_3) + (x - x_1)\,(x - x_2)] \tag{24}$$

  is positive, negative, and positive at $x = x_1$, $x = x_2$, and $x = x_3$, respectively. It follows that a graph of $x$ versus $\varphi$ can either oscillate between $x_1$ and $x_2$, or it can move away from $x_3$ towards infinity (which corresponds to $r \to 0$). If $x_1 < 0$, only part of an *oscillation* will actually occur. This corresponds to the particle coming from infinity, getting near the central mass, and then moving away again toward infinity, like the hyperbolic trajectory in the Newtonian case.

- $\boldsymbol{x_1 < x_2 = x_3}$: if the particle has just the right amount of energy (for a given angular momentum), $x_2$ and $x_3$ will merge. The radius $r_{\mathrm{in}} \sim 1/x_2 = 1/x_3$ is called the *inner radius*, and we have $3/2\,\rho \leqslant r_{\mathrm{in}} \leqslant 3\,\rho$. There are three solutions in this case:

  1. the orbit spirals into $r_{\mathrm{in}}$, approaching the inner radius (asymptotically) as a decreasing exponential in $\varphi$, $\tau$, or $t$, or
  2. one can have a circular orbit at the inner radius $r_{\mathrm{in}}$, or
  3. one can have an orbit that spirals down from the inner radius $r_{\mathrm{in}}$ towards the central singularity.

  Since $\mathrm{sn}\,(z,\, 1) = \tanh\,(z)$, in this case Eq. (22) simplifies to

$$x\,(\varphi) = x_1 + (x_2 - x_1)\tanh^2\left(\frac{\varphi}{2}\,\sqrt{\rho\,(x_2 - x_1)} + \delta\right)\ . \tag{25}$$

- $\boldsymbol{x_1 = x_2 < x_3}$: a circular orbit also results when $x_1 = x_2$. In this case, the radius $r_{\mathrm{out}} \sim 1/x_1 = 1/x_2$, is called the *outer radius*.

- $\boldsymbol{x_2\,,\, x_3 \in \mathbb{C}}$: if the particle approaches the center with enough energy and sufficiently low angular momentum then only $x_1$ will be real. This corresponds to the particle spiraling and falling into a black hole with a finite change in $\varphi$.

Equivalent forms of the above solutions are briefly reviewed in Appendix A.

## III. THE CENTRAL MASS AS A RANDOM VARIABLE

We shall now consider the mass $M$ as a random variable, assumed to be normally distributed with mean value $M_0$ and standard deviation $\sigma_M$ (the variance is $\sigma_M^2$) [30]. Equivalently, we may denote the mass $M$ as $M_0 + \delta M$, where $\delta M$ is a random variable with zero mean value, $\mu_{\delta M} = 0$, and variance $\sigma_M^2$, that is

$$\delta M \sim \mathcal{N}\left(0, \sigma_M^2\right) \ , \tag{26}$$

where $\mathcal{N}\left(\mu_z, \sigma_z^2\right)$ is the normalised Gaussian distribution of mean value $\mu_z$.

Since $\delta M$ is a random variable, any trajectory parametrised as $r = r(\varphi)$, will be a functional of this random variable which, for a given value of the angle $\varphi$, will therefore become a random variable itself. In order to stress that the angle $\varphi$ is now seen as a parameter, and $\delta M$ is treated as an independent (random) variable, we shall employ the notation $r = r_\varphi(\delta M)$.

Since Eq. (12) has the known analytical solution (22), it is conceivable to carry out the analysis of the probability distribution of $r_\varphi$, representing the position of the particle at a given angle $\varphi$, without relying on any perturbation methods.

In order to show explicitly the dependence on the mass $M$, we first rewrite Eq. (21) [equivalent to Eq. (12)] as

$$\left(\frac{\mathrm{d}u}{\mathrm{d}\varphi}\right)^2 = \frac{\rho}{M}\left(u - u_1\right)\left(u - u_2\right)\left(u - u_3\right) \ , \tag{27}$$

where we introduced the (dimensionful) variable

$$u = M\, x = \frac{L^2}{G\, r} \ , \tag{28}$$

and $u_i = M\, x_i$, for $i = 1, 2, 3$. The solution of Eq. (27) [equivalent to the solution (22)] is now given by

$$u(\varphi) = u_1 + \left(u_2 - u_1\right) \mathrm{sn}^2\left(\frac{\varphi}{2}\sqrt{\frac{\rho}{M}\left(u_3 - u_1\right)} + \delta,\, k\right) \ , \tag{29}$$

where

$$k = \sqrt{\frac{u_2 - u_1}{u_3 - u_1}}, \tag{30}$$

and $u(\varphi_0) = u_0$. It is important to remark that $u_1$, $u_2$, $u_3$, $\delta$, $\rho$ and $k$ are now all functions of $M$. Since we are assuming $M$ to be a random variable with a given probability density function $f_M$, the variable $u_\varphi \equiv u(\varphi)$ will turn into a random variable with probability distribution $f_{U_\varphi}$.

As customary in probability theory, from now on we shall indicate the random variables with capital letters ($M$ and $U_\varphi$, respectively for the mass and the dependent variable $u_\varphi$) and with lowercase letters ($m$ and $u_\varphi$, respectively), the values taken on by the random variables. We can therefore write Eq. (27) as

$$U_\varphi = u_1 + \left(u_2 - u_1\right) \mathrm{sn}^2\left(\frac{\varphi}{2}\sqrt{\frac{2\, G^2\, M}{L^2}\left(u_3 - u_1\right)} + \delta,\, k\right) \ . \tag{31}$$

In order to determine the probability density function $f_{U_\varphi}$ of the random variable $U_\varphi$, it is useful to work with its cumulative distribution function $\mathcal{F}_{U_\varphi}(u_\varphi)$, defined as the probability $\mathcal{P}$ of $U_\varphi$ taking on values smaller then or equal to $u_\varphi$. Since $U_\varphi$ is a monotonically increasing function of $M$ (which we shall denote with the symbol $g$, $U_\varphi = g(M)$), we have

$$\begin{aligned}
\mathcal{F}_{U_\varphi}(u_\varphi) &= \mathcal{P}(U_\varphi \leqslant u_\varphi) = \mathcal{P}(0 \leqslant M \leqslant m) \\
&= \int_0^m f_M(\xi)\, \mathrm{d}\xi \\
&= \int_0^{g^{-1}(u_\varphi)} f_M(\xi)\, \mathrm{d}\xi \ ,
\end{aligned} \tag{32}$$

where $u_\varphi = g(m)$. Making use of the fundamental theorem of calculus, we obtain

$$\begin{aligned} f_{U_\varphi}(u_\varphi) &= \frac{\mathrm{d}\mathcal{F}_{U_\varphi}(u_\varphi)}{\mathrm{d}u_\varphi} = \frac{\mathrm{d}\mathcal{F}_{U_\varphi}(u_\varphi)}{\mathrm{d}g^{-1}(u_\varphi)} \frac{\mathrm{d}g^{-1}(u_\varphi)}{\mathrm{d}u_\varphi} \\ &= f_M(m) \frac{\mathrm{d}g^{-1}(u_\varphi)}{\mathrm{d}u_\varphi} \\ &= \frac{f_M(m)}{g'(m)} = \frac{f_M(m)}{|g'(m)|} \ . \end{aligned} \tag{33}$$

Were the function $g$ monotonically decreasing, the previous derivation could be repeated just changing the sign of the inequality, that is

$$\begin{aligned} \mathcal{F}_{U_\varphi}(u_\varphi) &= \mathcal{P}(U_\varphi \leqslant u_\varphi) = \mathcal{P}(M > m) \\ &= \int_m^\infty f_M(\xi)\,\mathrm{d}\xi \\ &= -\int_\infty^{g^{-1}(u_\varphi)} f_M(\xi)\,\mathrm{d}\xi \ , \end{aligned} \tag{34}$$

which would lead to

$$f_{U_\varphi}(u_\varphi) = -\frac{f_M(m)}{g'(m)} = \frac{f_M(m)}{|g'(m)|} \ . \tag{35}$$

The case of a non-monotonic function $g$ can be treated similarly, just splitting the integration range so as to have a monotonic function in each interval. It is then easy to see that, if the function $f_{U_\varphi}$ has $N$ roots, which we denote as $u_\varphi = g(m_k)$, for $k = 1, 2, \ldots, N$, we obtain the general formula

$$f_{U_\varphi}(u_\varphi) = \sum_{k=1}^{N} \frac{f_M(m_k)}{|g'(m_k)|} \ , \tag{36}$$

The validity of the previous relation is not limited to $U_\varphi$ and $M$. In order to stress this, and for future use, the previous relation can be written as

$$f_Y(y) = \sum_{k=1}^{N} \frac{f_X(x_k)}{|g'(x_k)|} \ , \tag{37}$$

for a generic random variable $Y$ function of $X$ (with whatever probability density function $f_X$), such that $Y = g(X)$.

It is possible to extend the idea described above and to assume other parameters as random variables as well, not just the mass $M$. For instance, the initial position $u_0$ of the particle can be assumed as a random variable. In such a case, Eq. (37) can be applied, where the dependent and independent random variables are $U_\varphi$ and $U_0$, respectively, and $U_\varphi = g(U_0)$.

The next step, is to assume more parameters simultaneously as random variables. For example, the energy $E$ and the angular momentum $L$ might actually be considered as random variables with mean values equal to their nominal values (say $\mu_E$ and $\mu_L$, respectively) and variances accounting for their uncertainties (say $\sigma_E^2$ and $\sigma_L^2$, respectively). The random variables $E$ and $L$ would be in this case independent and follow normal distributions, $E \sim \mathcal{N}\left(\mu_E, \sigma_E^2\right)$, $L \sim \mathcal{N}\left(\mu_L, \sigma_L^2\right)$. In this case it is also conceivable that the variables $E$ and $L$ are not independent. In this scenario, it could be more accurate to introduce a joint probability density function $f_{EL}(e, l)$, instead of two independent probability density functions $f_E(e)$ and $f_L(l)$ for the energy and angular momentum separately. This approach is of course more general, and the case of independent variables could be recovered when $f_{EL}(e, l) = f_E(e)\, f_L(l)$.

This idea can be generalised even further. If the energy $E$, the angular momentum $L$, and the initial position $u_0$ are all affected by uncertainties and should be treated as random variables, we could have a joint probability density function $f_{ELU_0}(e, l, u_0)$. In all these cases, the variable $U_\varphi$ representing the quantity $u$ at some angle $\varphi$ would be a multivariate random variable, i.e. a function of more than one random variable. We shall continue to use the symbol $g$ for this function. However, a straightforward generalisation of Eq. (37) to this case does not appear possible.

In the case of two random variables, say $E$ and $L$, with joint probability density function $f_{EL}$, a procedure similar to the one presented for the case where $M$ is treated as a random variable would yield

$$\begin{aligned} \mathcal{F}_{U_\varphi}(u_\varphi) &= \mathcal{P}(U_\varphi \leqslant u_\varphi) = \mathcal{P}\left(g(E, L) \leqslant u_\varphi\right) \\ &= \int_{\mathcal{D}(u_\varphi)} f_{EL}(\xi, \eta)\,\mathrm{d}\xi\,\mathrm{d}\eta \ , \end{aligned} \tag{38}$$

where $\mathcal{D}(u_\varphi) \subset \mathbb{R}^2$ is the region of the $EL$ plane over which $g(E, L) \leqslant u_\varphi$. Once the cumulative distribution function $\mathcal{F}_{U_\varphi}(u_\varphi)$ is known, the probability density function $f_{U_\varphi}(u_\varphi)$ can be finally obtained by means of the definitions of $\mathcal{F}_{U_\varphi}$ and $f_{U_\varphi}$, i.e.

$$f_{U_\varphi}(u_\varphi) = \frac{\mathrm{d}\mathcal{F}_{U_\varphi}(u_\varphi)}{\mathrm{d}u_\varphi} \ . \tag{39}$$

In contrast with the case of a single random variable, this procedure for obtaining $f_{U_\varphi}(u_\varphi)$ is unlikely to be feasible analytically, due to the complexity of both the function $g$ and the domain of integration $\mathcal{D}$. It can probably be done numerically, though.

Following this approach, it should be possible to investigate the uncertainty on the orbit, described by a random variable $U_\varphi$, due to the uncertainties on the parameters $E$, $L$, $U_0$ (and possibly others), and to compare this uncertainty on the orbit to the one produced by an uncertainty of the central mass $M$. The basis of this approach is laid on two key ingredients:

1. Finding the (analytical or numerical) solution of the equation of motion (13);
2. Computing the probability density function of the orbit, once the probability density functions of the parameters are given, following the method described above.

## IV. MASS UNCERTAINTY AND NON-CIRCULAR ORBITS

In Section II B 2, solutions of the equation of motion (2) were reviewed, and qualitatively different kinds of orbit have been identified. For these orbits, the effect of assuming the mass $M$ as a normally distributed random variable is now investigated for orbits with set initial conditions for the position and velocity. Let us first recall that we shall be using the (dimensionful) variable $u$ in Eq. (28), like in the previous Section, and that the orbits are divided into the following four groups ($u_0$ represents the initial position of the particle):

- If the third degree polynomial on the right-hand side of Eq. (27) has three distinct real roots ($u_1 < u_2 < u_3$), we can have the following behaviours:
  - if $0 < u_1 < u_0 < u_2 < u_3$, the graph of $u$ versus $\varphi$ oscillates between $u_1$ and $u_2$ (**first case**);
  - if $0 < u_1 < u_2 < u_3 < u_0$ , the graph of $u$ versus $\varphi$ moves away from $u_3$ towards infinity (**second case**);
  - if $u_1 < 0 < u_0 < u_2 < u_3$ only part of an oscillation occurs, with the particle first approaching the central mass and then moving away towards infinity (**third case**);
- If the polynomial has one real root and two complex conjugates roots, the particle falls into the black hole and the orbit is a spiral with a finite change in $\varphi$ (**fourth case**).

It is important to recall that, if the energy and the angular momentum of the particle are such that $u_1 < u_2 = u_3$, three behaviours are possible: the orbit may be circular at the radius $r_{\text{in}} \sim 1/u_2 = 1/u_3$ (the inner radius), or it may spiral in asymptotically approaching the inner radius or spiral down from the inner radius to the central point. If instead $u_1 = u_2 < u_3$, a circular orbit at the radius $r_{\text{out}} \sim 1/u_1 = 1/u_2$ (the outer radius) is also possible. In all of these cases, after the slightest perturbation of the central mass $M$, we fall back in one of the four previous cases. For example, when the stable orbit is perturbed, we fall in the first case.

In the following, we shall analyse the above four cases. For the purpose of making the results more readable, we will first show plots of the orbits corresponding to fixed numerical values of the parameters of relevance for the each distribution of the mass $M$, and specifically chosen for the purpose of displaying clearly the qualitative features of the orbits in the case under consideration. We then display the chosen distribution for the mass $M$ and the final distribution of the quantity of relevance again for each specific case (*e.g.* amplitude of the oscillation, minimum distance from the centre, etc). In particular, we shall use units with $G = 1$.

### A. First case

When the orbit oscillates between $u_1$ and $u_2$, it is interesting to analyse the amplitude $A$ (and the period) of the oscillations as a function of the random variable $M$. For example, the trajectories $r = r(\varphi)$ corresponding to three different values of $M$ are shown in Fig. 1 in polar form. Cartesian plots of $u(\varphi)$ are shown in Fig. 2, together with

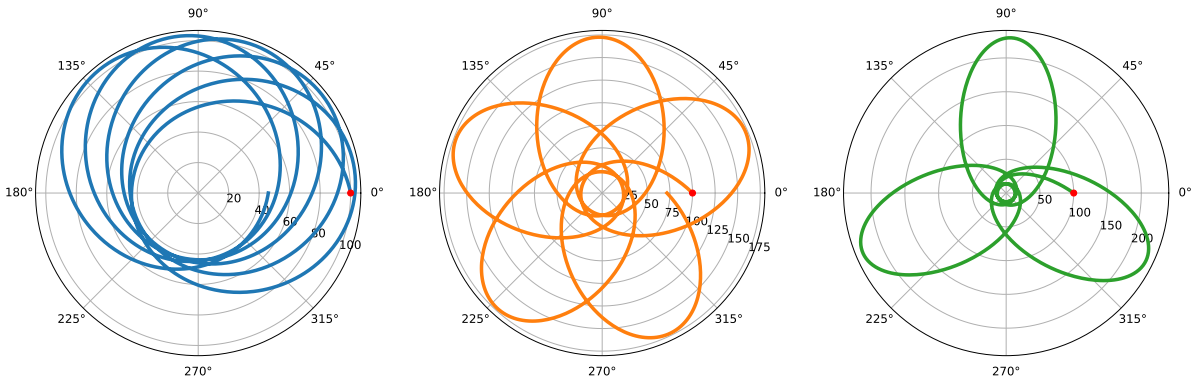



FIG. 1. (First case) Orbits for different values of $M = 1.5$, 2, 2.5 (left to right, with $G = 1$, $E = 0.9$, $L = 10$, $u_0 = 1$.) The red dot is the starting point and colours are the same as in Fig. 2.

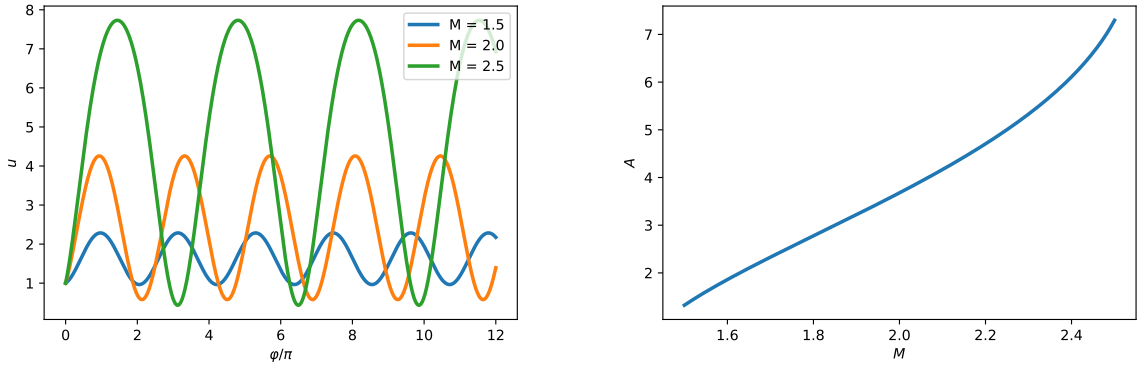



FIG. 2. (First case) Graphs of $u(\varphi)$ for different values of $M = 1.5$, 2, 2.5 (with $G = 1$, $E = 0.9$, $L = 10$, $u_0 = 1$) (left panel), and maximum amplitude of the oscillations as a function of the mass $M$ (right panel).

the amplitude of the oscillations $A$, as a function of the mass $M$. (When comparing Fig. 1 with Fig. 2, it should be noted that $r = L^2/G\,u = 100/u$.)

If the random variable $M$ is normally distributed with mean value $\mu_M = 1.5$ and standard deviation $\sigma_M = 0.1$, the probability density function $f_A$ of the random variable $A$ can be obtained by means of Eq. (37) once the probability density function $f_M$ and the function $A = g(M)$ are known. The probability density functions $f_M$ and $f_A$ are shown in Fig. 3.

### B. Second case

The second possibility listed above is that the particle will monotonically move towards the central mass ($u \to \infty$), as is shown by the polar trajectories $r(\varphi)$ represented in Fig. 4. For such a type of orbits, the function $u\,(\varphi)$ is plotted for several values of $M$ in Fig. 5. For this case, it is therefore interesting to analyse the behaviour of $u_\varphi$ as a function of $M$ for different values of the angle $\varphi$ that parameterizes the orbit.

If the random variable $M$ is normally distributed with mean value $\mu_M = 1$ and standard deviation $\sigma_M = 0.05$, the resulting probability density function $f_U$ of the random variable $u_\varphi$, for some exemplary values of $\varphi$, is shown in Fig. 6 along with the corresponding probability density function $f_M$. As expected the variance of the probability density function of $u_\varphi$ increases with $\varphi$.

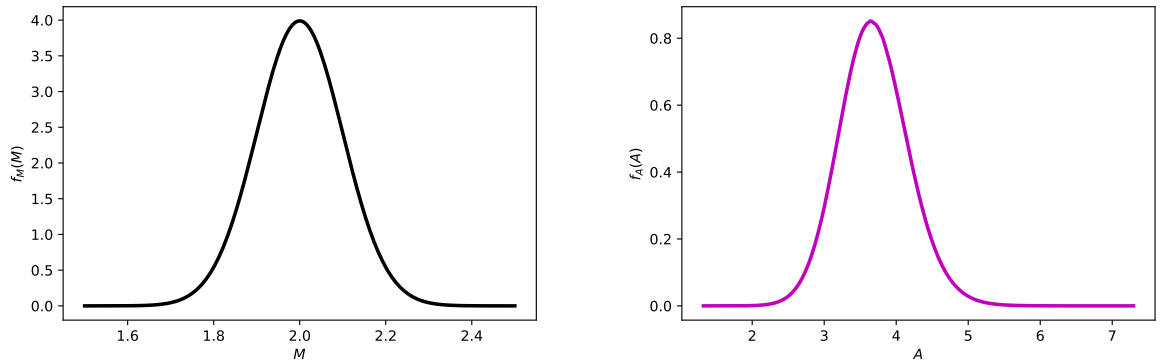



FIG. 3. (First case) Probability density function for the mass $M$ (left panel) and for the amplitude $A$ (right panel). The amplitude corresponding to the mean value of $M$ is $\sim 3.68$; the value of the amplitude corresponding to the maximum of the distribution of $A$ if $\sim 3.64$. (The random variable $A$ is not normally distributed, and its distribution is not symmetric).

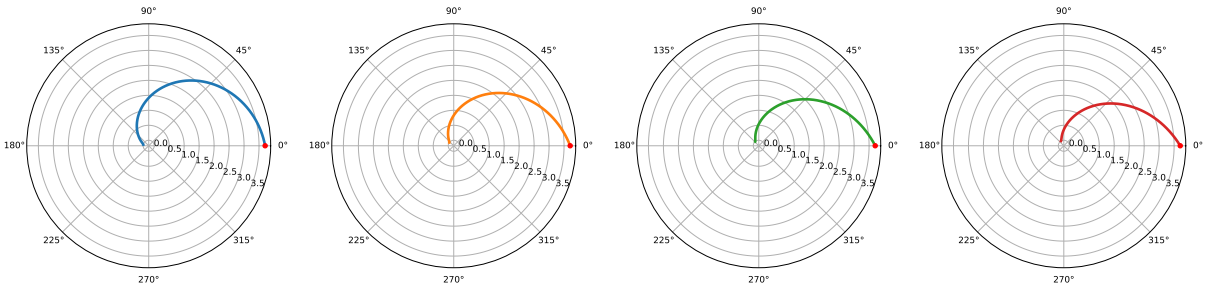


FIG. 4. (Second case) Orbits for values of $M = 1.7, 1.9, 2.1, 2.3$ (left to right, with $G = 1$, $E = 0.99$, $L = 10$, $u_0 = 27$.) The red dot is the starting point and colours are the same as in Fig. 5(a).

### C. Third case

Another type of solution is the one representing a particle coming from infinity towards the central mass and then moving back towards infinity ($r \to \infty$, i.e. $u \to 0$). Some typical polar trajectories $r(\varphi)$ of this kind are shown in Fig. 7 and the corresponding function $u(\varphi)$ are displayed in Fig. 8. The maximum value $D$ of $u$ reached along the trajectory (proportional to the inverse of the minimum distance from the central mass) is also plotted as a function of $M$.

If the random variable $M$ is normally distributed with mean value $\mu_M = 1$ and standard deviation $\sigma_M = 0.2$, the probability density function $f_D$ of the random variable $D$ is again obtained by means of Eq. (37). The probability density functions $f_M$ and $f_D$ are shown in Fig. 9.

### D. Fourth case

The last type of solution is the one representing a particle with enough energy and sufficiently low angular momentum which spirals into a black hole with a finite change in $\varphi$. Some examples of these orbits are shown in Fig. 10 and the corresponding function $u(\varphi)$ is plotted in Fig. 11, along with the behaviour of $u_\varphi$ as a function of $M$ for different values of the angle $\varphi$.

For $M$ normally distributed with mean value $\mu_M = 2.2$ and standard deviation $\sigma_M = 0.05$, the resulting probability density functions $f_U$ for some angles $\varphi$ is shown in Fig. 12.

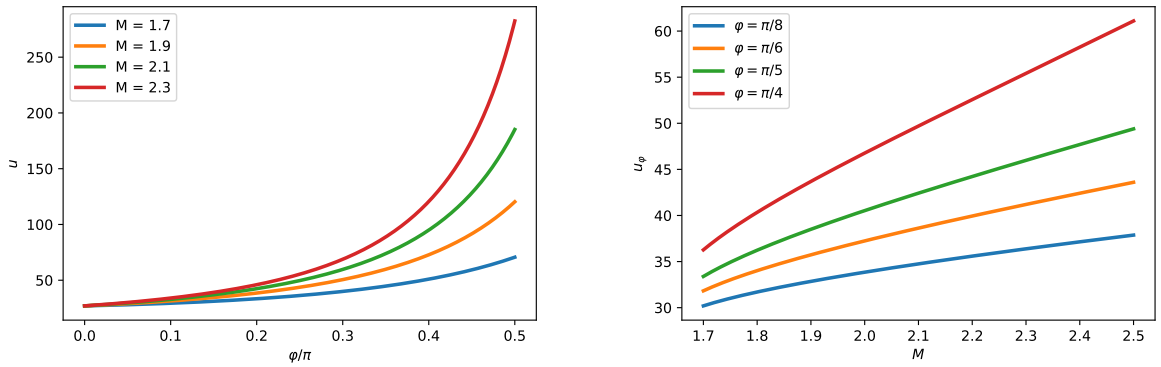



FIG. 5. (Second case) Graphs of $u(\varphi)$ for values of $M = 1.7, 1.9, 2.1, 2.3$ (left panel, with $G = 1$, $E = 0.99$, $L = 10$, $u_0 = 27$), and $u_\varphi$ as a function of the mass $M$ for fixed angles $\varphi$ (right panel).

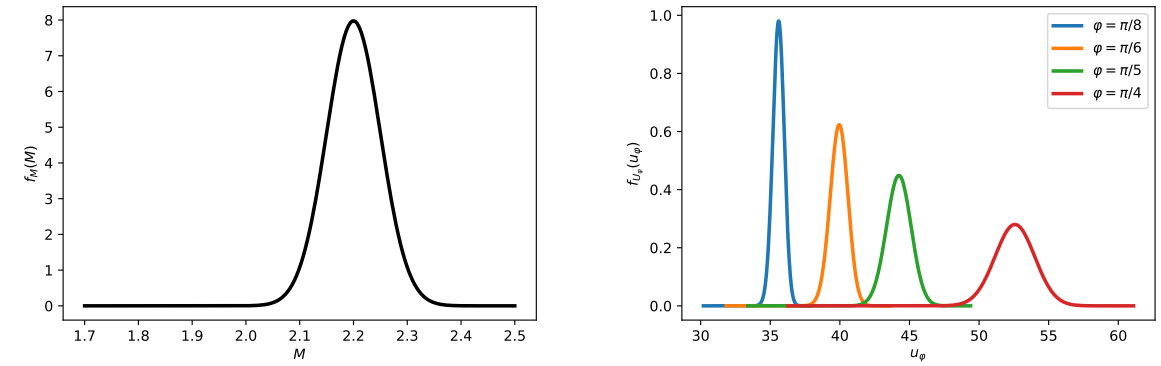



FIG. 6. (Second case) Probability density function for the mass $M$ (left panel) and for the variable $u_\varphi$ for different angles $\varphi$ (right panel).

## V. PERTURBATION OF CIRCULAR ORBITS

We can now study circular orbits again using the variable $u$ defined in Eq. (28), so that Eq. (12) reads

$$\left(\frac{\mathrm{d}u}{\mathrm{d}\varphi}\right)^2 = \frac{E^2\,L^2}{G^2} - \varepsilon\,\frac{L^2}{G^2} + 2\,\varepsilon\,M\,u - u^2 + \gamma\,\frac{2\,G^2\,M}{L^2}\,u^3 \tag{40}$$

and Eq. (13) reads

$$\frac{\mathrm{d}^2u}{\mathrm{d}\varphi^2} = \varepsilon\,M - u + \gamma\,\frac{3\,G^2\,M}{L^2}\,u^2\ . \tag{41}$$

We wish to study the effect on circular orbits of small perturbations affecting the central mass $M$ and the initial position of the test particle. We shall first use an analytical perturbative approach for Eq. (41) with the initial conditions

$$u(0) = u_\mathrm{c} \equiv \frac{L^2}{G\,r_c}\ , \qquad \frac{\mathrm{d}u}{\mathrm{d}\varphi}(0) = 0\ , \tag{42}$$

where $r_\mathrm{c}$ is the radius of a circular orbit (either internal or external). Note that the initial condition on the derivative implies that an instantaneous perturbation of the mass does not instantaneously alter the tangential component of the particle velocity.

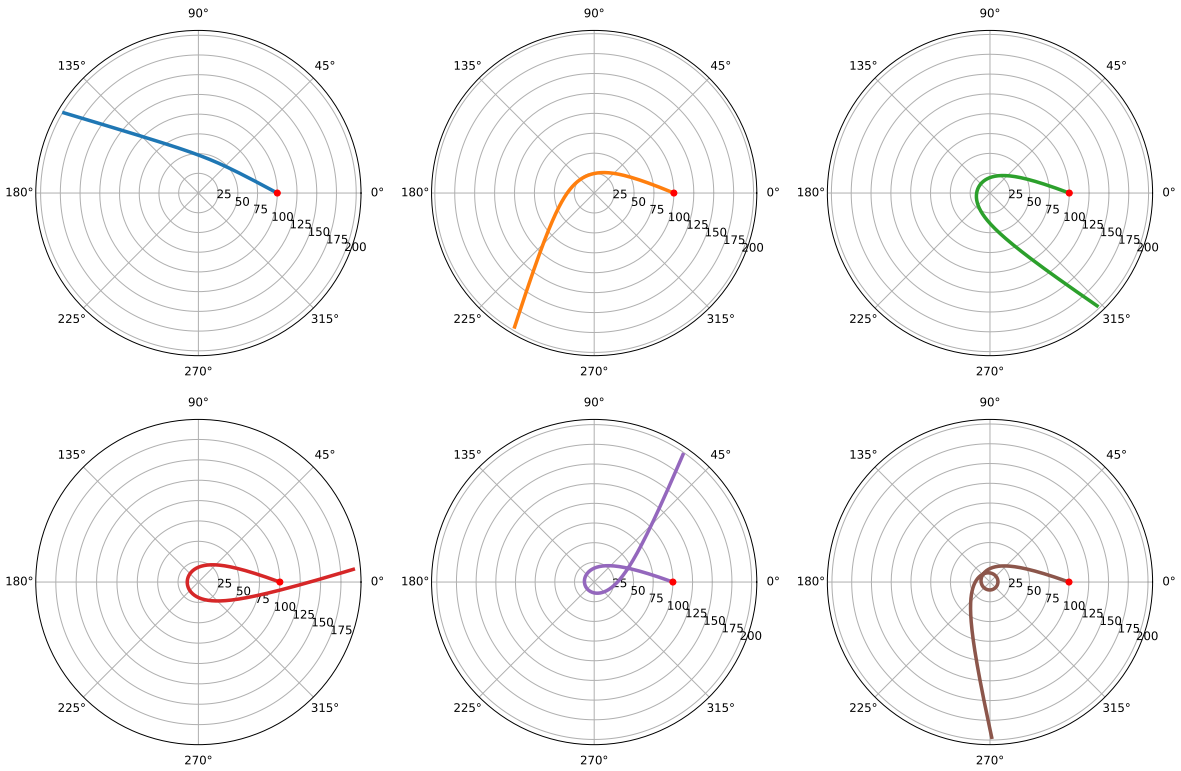



FIG. 7. (Third case) Orbits for values of $M$ ranging from 0.2 to 2.4 (tope left to bottom right, with $G = 1$, $E = 1.02$, $L = 10$, $u_0 = 1$.) The red dot is the starting point and colours are the same as in Fig. 8.

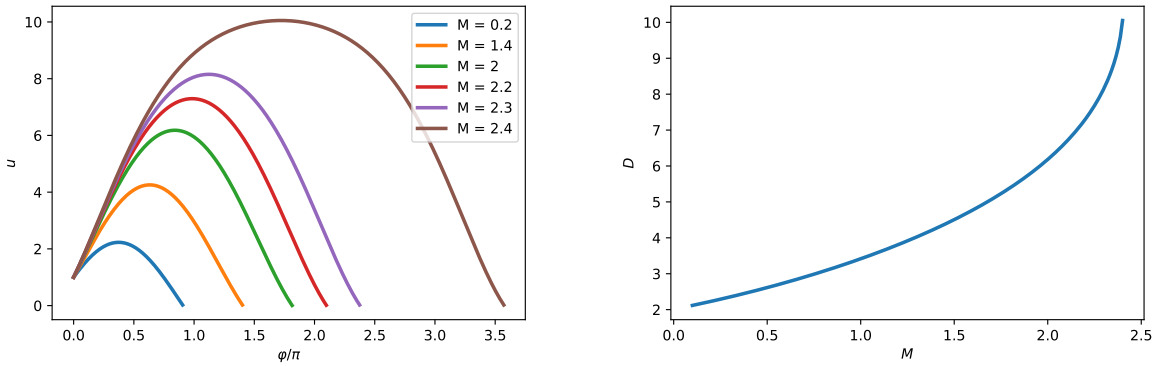



FIG. 8. (Third case) Graphs of $u(\varphi)$ for values of $M$ ranging from 0.2 to 2.4 (left panel, with $G = 1$, $E = 1.02$, $L = 10$, $u_0 = 1$) and maximum value $D$ of $u$ (inverse minimum distance of the particle from the central mass) as a function of the mass $M$ (right panel).

### A. Mass perturbation

If we denote with $\delta M$ the perturbation on the mass $M$, the perturbed solution can be written as

$$u = u^{(0)} + \frac{\delta M}{M}\, u^{(1)} + \mathcal{O}\left(\frac{\delta M^2}{M^2}\right) \ . \tag{43}$$

Upon replacing into Eq. (41) and keeping terms up to order $\delta M/M$, we find

$$\frac{\mathrm{d}^2 u^{(0)}}{\mathrm{d}\varphi^2} + \frac{\delta M}{M}\frac{\mathrm{d}^2 u^{(1)}}{\mathrm{d}\varphi^2} = \varepsilon\,(M+\delta M) - u^{(0)} - \frac{\delta M}{M}\,u^{(1)} + \gamma\,\frac{3\,G^2}{L^2}\,(M+\delta M)\left(u^{(0)} + \frac{\delta M}{M}\,u^{(1)}\right)^2 \ . \tag{44}$$

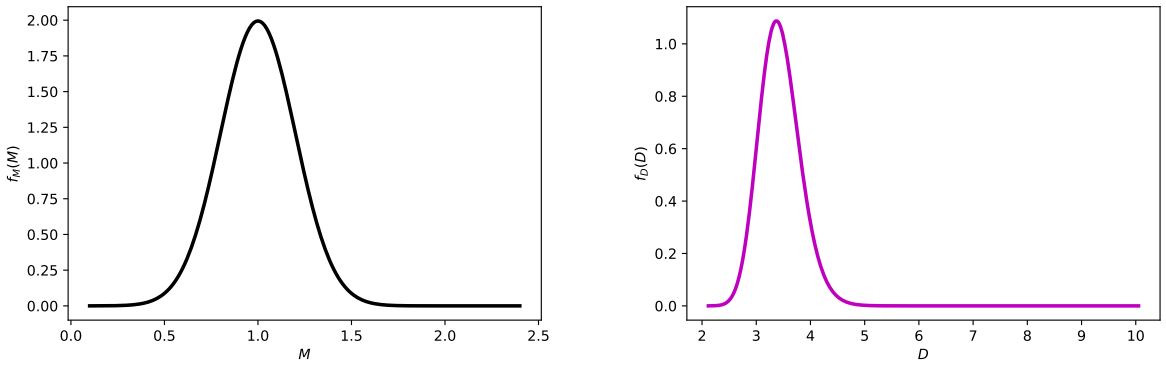



FIG. 9. (Third case) Probability density function for the mass $M$ (left panel) and for the amplitude $D$ inversely proportional to the minimum distance from the central mass (right panel).

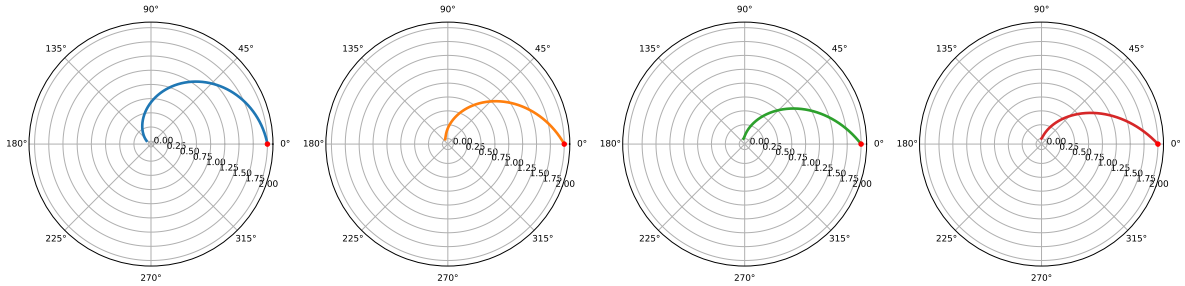


FIG. 10. (Fourth case) Orbits for values of $M = 1$, 1.3, 1.6, 1.9 (left to right, with $G = 1$, $E = 0.98$, $L = 10$, $u_0 = 50$. The red dot is the starting point and colours are the same as in Fig. 11.

Assuming $u^{(0)}$ satisfies the unperturbed equation (2) with fixed $M$, we obtain that the first order correction must satisfy

$$\frac{\mathrm{d}^2 u^{(1)}}{\mathrm{d}\varphi^2} = \alpha_c \, u^{(1)} + \beta_c \ , \tag{45}$$

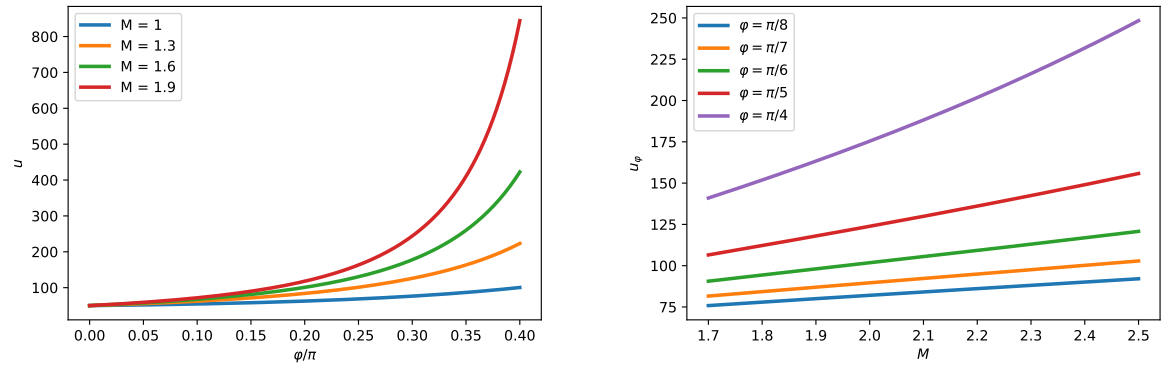



FIG. 11. (Fourth case) Graphs of $u(\varphi)$ for values of $M = 1$, 1.3, 1.6, 1.9 (left panel, with $G = 1$, $E = 0.98$, $L = 10$, $u_0 = 50$) and maximum value $D$ of $u$ (inverse minimum distance of the particle from the central mass) as a function of the mass $M$ (right panel) .

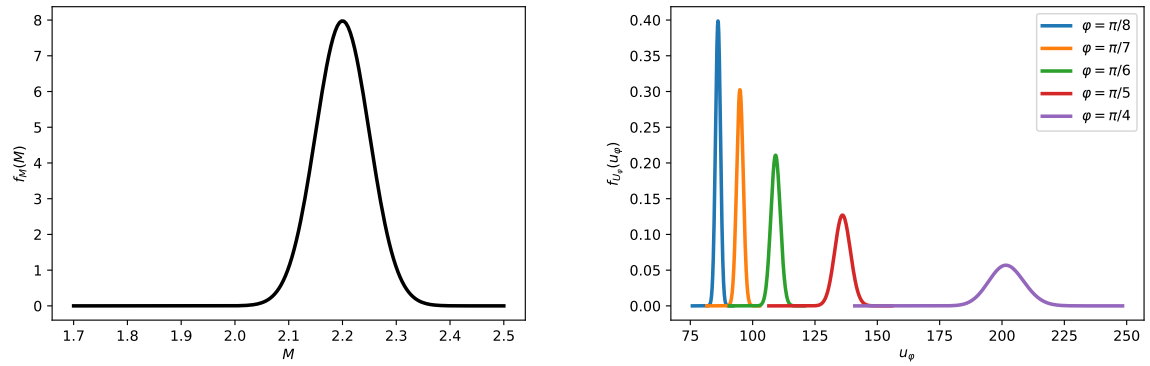



FIG. 12. (Fourth case) Probability density function for the mass $M$ (left panel) and for the amplitude $U$ (right panel).

where

$$\alpha_{\rm c} \equiv \gamma \, \frac{6\,G^2\,M}{L^2}\, u^{(0)} - 1 \tag{46}$$

and

$$\beta_{\rm c} \equiv \gamma \, \frac{3\,G^2\,M}{L^2} \left(u^{(0)}\right)^2 + \varepsilon\, M \ . \tag{47}$$

Moreover, the initial conditions for $u^{(1)}$ are given by

$$u^{(1)}(0) = \frac{{\rm d}u^{(1)}}{{\rm d}\varphi}(0) = 0 \ . \tag{48}$$

Focusing on the case $\gamma = 1$, and restricting ourselves, from now on, to the perturbation of circular orbits ($u^{(0)} = u_{\rm c}$), we treat the massive and massless cases separately.

In the massive case ($\varepsilon = 1$), two circular orbits exist [see Eq. (7)]:

1. For the internal orbit we have $r_c = r_{\rm in} = r_-$ in Eq. (7), that is

$$u_c = u_{\rm in} = \frac{L^2 + \sqrt{L^4 - 12\,G^2\,M^2\,L^2}}{6\,G^2\,M} \ , \tag{49}$$

for which $\alpha_{\rm c} = \alpha > 0$ [see Eq. (7)] and $\beta_{\rm c} = u_{\rm in}$. The analytical solution of Eq. (45) is then

$$u^{(1)} = \frac{\beta_c}{\alpha_c} \left[\cosh\left(\sqrt{\alpha_c}\,\varphi\right) - 1\right] \ , \tag{50}$$

and it is easy to see that, as expected, this orbit is unstable. In fact, the perturbed solution (43) to first order reads

$$u(\varphi) \simeq u_{\rm in} \left[1 + \frac{\delta M}{M}\, \frac{\cosh\left(\sqrt{\alpha}\,\varphi\right) - 1}{\alpha}\right] \ , \tag{51}$$

from which we can see that increasing the mass ($\delta M > 0$) leads to $r \to 0$ ($u \to \infty$). On the other hand, reducing the mass ($\delta M < 0$), leads to $r \to \infty$ ($u = 0$) for some finite value of $\varphi$.

2. For the external orbit we have $r_c = r_{\rm out} = r_+$ in Eq. (7), or

$$u_c = u_{\rm out} = \frac{L^2 - \sqrt{L^4 - 12\,G^2\,M^2\,L^2}}{6\,G^2\,M} \ , \tag{52}$$

so that $\alpha_{\rm c} = -\alpha < 0$ and $\beta_{\rm c} = u_{\rm out}$. The analytical solution of Eq. (45) is now

$$u^{(1)} = \frac{\beta_c}{\alpha_c} \left[\cos\left(\sqrt{|\alpha_c|}\,\varphi\right) - 1\right] \ , \tag{53}$$

which implies that the outer orbit is stable, with $u^{(1)}$ oscillating between 0 and $2\,\beta_{\rm c}/\left|\alpha_{\rm c}\right|$. The perturbed solution to first order is given by

$$u(\varphi) \simeq u_{\rm out}\left[1+\frac{\delta M}{M}\,\frac{1-\cos\left(\sqrt{\alpha}\,\varphi\right)}{\alpha}\right]\,, \tag{54}$$

so that $\delta M > 0$ leads to periodic oscillations internal ($u \geq u_{\rm out}$) to the stable orbit $r = r_{\rm out}$, whereas $\delta M < 0$ leads to periodic oscillations external ($u \leq u_{\rm out}$) to the stable orbit $r = r_{\rm out}$. This is potentially quite interesting in practical terms because the oscillations are proportional to the perturbation $\delta M$ (assuming that the oscillations are large enough to be detectable).

For the massless case ($\varepsilon = 0$), there is one possible circular orbit $r_{\rm c} = r_{\rm ph}$ in Eq. (6), or

$$u_{\rm c} = u_{\rm ph} = \frac{L^2}{3\,G^2\,M}\,. \tag{55}$$

In this case Eq. (45) becomes

$$\frac{{\rm d}^2u^{(1)}}{{\rm d}\varphi^2} = u^{(1)} + u_{\rm ph} \tag{56}$$

and its analytical solution is

$$u^{(1)} = u_{\rm c}\left[\cosh(\varphi)-1\right]\,. \tag{57}$$

It is clear that, since $u^{(1)} \to \infty$ as $\varphi \to \infty$, the orbit

$$u(\varphi) \simeq u_{\rm ph}\left\{1+\frac{\delta M}{M}\left[\cosh(\varphi)-1\right]\right\} \tag{58}$$

is unstable, and it will fall into the singularity ($u \to \infty$) if $\delta M > 0$ or escape to infinity ($u \to 0$) if $\delta M < 0$.

### B. Initial position perturbation

Let us now consider a perturbation $\delta u_0$ on the initial position $u_0$, so that

$$u = u^{(0)} + \frac{\delta u_0}{u_0}\,u^{(1)} + \mathcal{O}\left(\frac{\delta u_0^2}{u_0^2}\right)\,. \tag{59}$$

From Eq. (41), we have

$$\begin{aligned}\frac{{\rm d}^2u^{(0)}}{{\rm d}\varphi^2} + \frac{\delta u_0}{u_0}\,\frac{{\rm d}^2u^{(1)}}{{\rm d}\varphi^2} = \gamma\,\frac{3\,G^2\,M}{L^2}\left[\left(u^{(0)}\right)^2 + \frac{\delta u_0}{u_0}\left(u^{(1)}\right)^2 + 2\,\frac{\delta u_0}{u_0}\,u^{(0)}\,u^{(1)}\right] \\ +\varepsilon\,M - u^{(0)} - \frac{\delta u_0}{u_0}\,u^{(1)}\end{aligned} \tag{60}$$

so that the first order perturbation must satisfy

$$\frac{{\rm d}^2u^{(1)}}{{\rm d}\varphi^2} = \alpha_{\rm c}\,u^{(1)}\,, \tag{61}$$

with $\alpha_{\rm c}$ still given by Eq. (46). Moreover, the proper initial conditions are given by

$$u^{(1)}(0) = \delta u_0\,, \qquad \frac{{\rm d}u^{(1)}}{{\rm d}\varphi}(0) = 0\,. \tag{62}$$

Similarly to the case of mass perturbations, we shall only consider circular orbits ($u^{(0)} = u_{\rm c} = u_0$ and $\delta u_0 \equiv \delta u_{\rm c}$) for $\gamma = 1$ and distinguish the massive and massless cases.

In the massive case ($\varepsilon = 1$), we distinguish the internal and the external orbits:

| $\varepsilon$ | $u_{\rm c}$ | $u(\varphi;\delta M)$ | $u(\varphi;\delta u_0)$ |
|---|---|---|---|
| 1 | $u_{\rm in}$ in Eq. (49) | $u_{\rm in}\left[1+\frac{\delta M}{M}\,\frac{\cosh\left(\sqrt{\alpha}\,\varphi\right)-1}{\alpha}\right]$ | $u_{\rm in}\left[1+\frac{\delta u_{\rm c}}{u_{\rm in}}\,\cosh\left(\sqrt{\alpha}\,\varphi\right)\right]$ |
| 1 | $u_{\rm out}$ in Eq. (52) | $u_{\rm out}\left[1+\frac{\delta M}{M}\,\frac{1-\cos\left(\sqrt{\alpha}\,\varphi\right)}{\alpha}\right]$ | $u_{\rm out}\left[1+\frac{\delta u_{\rm c}}{u_{\rm out}}\,\cos\left(\sqrt{\alpha}\,\varphi\right)\right]$ |
| 0 | $u_{\rm ph}$ in Eq. (55) | $u_{\rm ph}\left\{1+\frac{\delta M}{M}\left[\cosh(\varphi)-1\right]\right\}$ | $u_{\rm ph}\left[1+\frac{\delta u_{\rm c}}{u_{\rm ph}}\,\cosh\left(\varphi\right)\right]$ |

TABLE I. Overview of perturbed solutions.

1. For the internal orbit $u_{\rm c}=u_{\rm in}$, we can write the perturbation as

$$u^{(1)}=\delta u_{\rm c}\cosh\left(\sqrt{\alpha_{\rm c}}\,\varphi\right)\ , \tag{63}$$

where $\alpha_{\rm c}=\alpha$. The perturbed solution

$$u(\varphi)\simeq u_{\rm in}\left[1+\frac{\delta u_{\rm c}}{u_{\rm in}}\,\cosh\left(\sqrt{\alpha}\,\varphi\right)\right] \tag{64}$$

is therefore unstable.

2. For the external orbit $u_{\rm c}=u_{\rm out}$, the perturbation is given by

$$u^{(1)}=\delta u_{\rm c}\,\cos\left(\sqrt{|\alpha_{\rm c}|}\,\varphi\right)\ , \tag{65}$$

with $\alpha_{\rm c}=-\alpha$. The perturbed solution reads

$$u(\varphi)=u_{\rm out}\left[1+\frac{\delta u_{\rm c}}{u_{\rm out}}\,\cos\left(\sqrt{\alpha}\,\varphi\right)\right]\ , \tag{66}$$

which is stable, with oscillations of amplitude $2\,\delta u_{\rm c}$ around the circular orbit.

For the massless case ($\varepsilon=0$), there is one possible circular orbit (6) with $u_{\rm c}=u_{\rm ph}=L^2/3\,G^2\,M$ and Eq. (61) reads

$$\frac{{\rm d}^2u^{(1)}}{{\rm d}\varphi^2}=u^{(1)}\ , \tag{67}$$

with solution

$$u^{(1)}=\delta u_{\rm c}\cosh\left(\varphi\right)\ . \tag{68}$$

As expected, the orbit is unstable,

$$u(\varphi)\simeq u_{\rm ph}\left[1+\frac{\delta u_{\rm c}}{u_{\rm ph}}\,\cosh\left(\varphi\right)\right]\ . \tag{69}$$

We can now easily compare the effect of a perturbation in the initial position with the one produced by a perturbation in the central mass by looking at Table I. It appears that the two effects are very similar, in fact, and in the following we shall focus on the first case in the table.

## VI. UNSTABLE CIRCULAR ORBITS

In this section we want to analyse more in details the unstable inner circular orbit $r_{\rm in}$ for massive particles. Since the analysis will be performed numerically, it is convenient to introduce the dimensionless variables

$$\tilde{L}\equiv\frac{L}{G\,M}\ ,\qquad \tilde{r}_{\rm in}\equiv\frac{r_{\rm in}}{G\,M}\ , \tag{70}$$

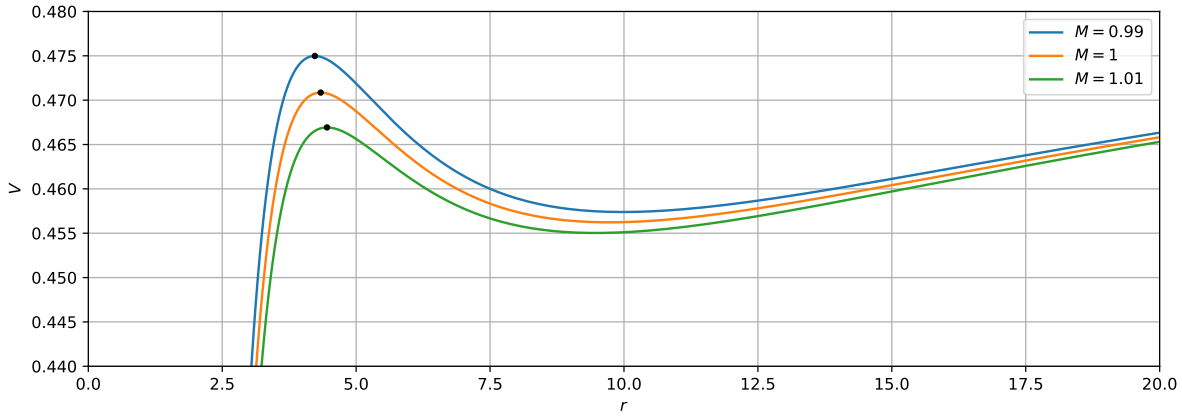



FIG. 13. Potential $V$ as a function of the radial coordinate $r$ for values of the central mass $M = 0.99, 1, 1.01$ (with $G = 1$, $L = 3.75$). Black dots represent the local maximum of the potential, corresponding to the unstable circular orbits.

and recall that (two) circular orbits exist under the condition $\tilde{L} \geq \sqrt{12}$. In particular, as discussed in Section II A 2, the inner radius

$$3 = \tilde{r}_{\rm in}(\tilde{L} \to \infty) \leq \tilde{r}_{\rm in} \leq \tilde{r}_{\rm in}(\tilde{L} = \sqrt{12}) = 6 \ . \tag{71}$$

Since the energy and the angular momentum of test particles moving on the internal circular orbits are connected by the relation

$$E = 108 \left[ 36 - \tilde{L}^{-1} \left( \tilde{L}^2 - 12 \right)^{3/2} + \tilde{L} \right] \ , \tag{72}$$

the effects of a perturbation of the mass $M$ can be determined by considering $L$ as the only free parameter.

It is worth noticing that, in our analysis, an instantaneous reduction of the mass $M$, i.e. a perturbation $\delta M < 0$, leads to a smaller radius for the circular orbit and to an increase of the corresponding potential $V$ (see Fig. 13). After the perturbation, the particle orbiting on the circular orbit would happen to have an energy lower than the potential energy $V$. We shall therefore consider only perturbations $\delta M > 0$, i.e. instantaneous increases of the mass $M$. (Note that in the analytical perturbation method, solutions are found under the condition $du/d\varphi(0) = 0$, see Eq. (42) and following comment.)

The change of the radial coordinate of the particle as a function of the angle $\varphi$ following an instantaneous perturbation $\delta M > 0$ are shown in Fig. 14, Fig. 15 and Fig. 16 for three values of the angular momentum, namely

1. $\tilde{L} = \sqrt{12}$, which is the minimum possible value for which the circular orbit exists. The radius of the circular orbit in this case is $\tilde{r}_{\rm in} = 6$ (Fig. 14);
2. $\tilde{L} = 4$, for which the radius of the circular orbit is $\tilde{r}_{\rm in} = 4$ (Fig. 15);
3. $\tilde{L} = 100$, for which the radius of the circular orbit is $\tilde{r}_{\rm in} \approx 3.0009$, close to the minimum possible value $\tilde{r}_{\rm in} = 3$ (Fig. 16).

For all the three cases analysed here, the radial position of the particle as a function of the number $N$ of revolutions ($N = \varphi/2\,\pi$) is shown for several values of the perturbation $\delta M/M$, ranging from $10^{-5}$ to $10^{-1}$. The results show that the number of revolutions after which the particle decrease its radial coordinate by 5% of the original value is always less than 2, and decreases as the perturbation increases or the angular momentum increases. For each of the three cases, the polar representations of the orbits are shown for three selected values of the perturbation, namely $\delta M/M = 10^{-5}, 10^{-3}, 10^{-1}$. The number of revolutions $N$ after which the variation of the radial position of the particle amounts to 5% of the initial value has then been systematically investigated for values of the perturbation parameter $\delta M/M$ varying between $10^{-6}$ and $10^{-1}$. The result is shown in Fig. 17.

Let us next assume the perturbation $\delta M > 0$ is a random variable with distribution $\mathcal{N}^*\left(\mu_{\delta M}, \sigma_{\delta M}\right)$, i.e. a random variable with probability density function

$$f_{\delta M}(x) = \begin{cases} 0 & x < 0 \\ \dfrac{2}{\sqrt{2\pi\sigma^2}} \exp\left[ -\dfrac{\left(x - \mu_{\delta M}\right)^2}{2\,\sigma_{\delta M}^2} \right] & x \geqslant 0 \ . \end{cases} \tag{73}$$

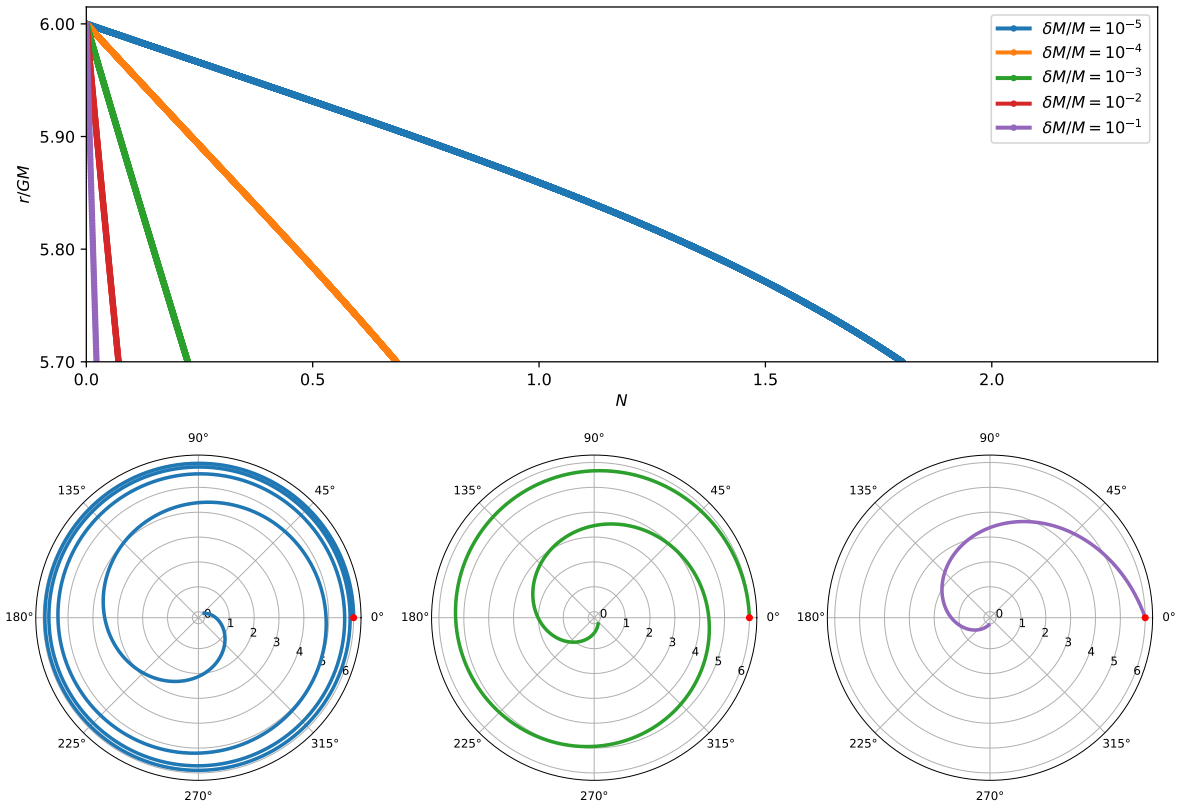



FIG. 14. Radial coordinate $\tilde{r} = r/G\,M$ of trajectories subject to perturbations $\delta M$ starting from the unstable circular orbit for $\tilde{L} = L/G\,M = \sqrt{12}$ (top panel); trajectories subject to the perturbation $\delta M/M = 10^{-5}$ (bottom left panel), $\delta M/M = 10^{-3}$ (bottom center panel) and $\delta M/M = 10^{-1}$ (bottom right panel).

Setting $\mu_{\delta M} = 0$ and $\sigma_{\delta M} = 0.0005$, the corresponding random variable representing the number of revolutions $N$ after which the variation of the radial coordinate amounts to 5% of the initial value is shown in Fig. 18. The same analysis for a ten times larger value of $\sigma_{\delta M} = 0.005$ is also shown in Fig. 19. The cumulative distribution functions of the random variable $N$ for the two cases $\sigma_{\delta M} = 0.0005$ and $\sigma_{\delta M} = 0.005$ are shown in Fig. 20.

## VII. DISCUSSION AND OUTLOOK

In this work we started to consider in detail the effects of uncertainties in the determination of the black hole mass on geodesics, mainly motivated by studies of quantum aspects of black holes [23–27]. In particular, we analysed the consequences of a randomly distributed mass on qualitatively different orbits and we were interested in the possible differences between such effects and those simply stemming from the experimental uncertainties in the measurements of masses and positions. It is in fact important to be able to tell apart the two sources of uncertainties if one eventually wishes to look for experimental evidence of quantum gravity in black hole physics.

A comparison between the two kinds of uncertainties for circular orbits was considered in Section V, where we showed that they appear functionally very similar, which points to the fact that it would be very difficult to identify quantum effects from experimental data [31] about such orbits of test bodies obtained, for instance, by the Event Horizon Telescope [32] and BlackHoleCam [33, 34]. In the search for more significant signatures of quantum effects, beside considering more explicitly models of quantum black holes [11–14, 35–38], we also intend to study other effects occurring on black hole space-times. In particular, it will be interesting to investigate the red-shift of signals emitted by sources either falling towards the black hole along (perturbed and unperturbed geodesics) as well as following perturbed unstable circular orbits. Given the precision with which the red-shift can be measured, this might be a more promising route towards experimental quantum gravity.

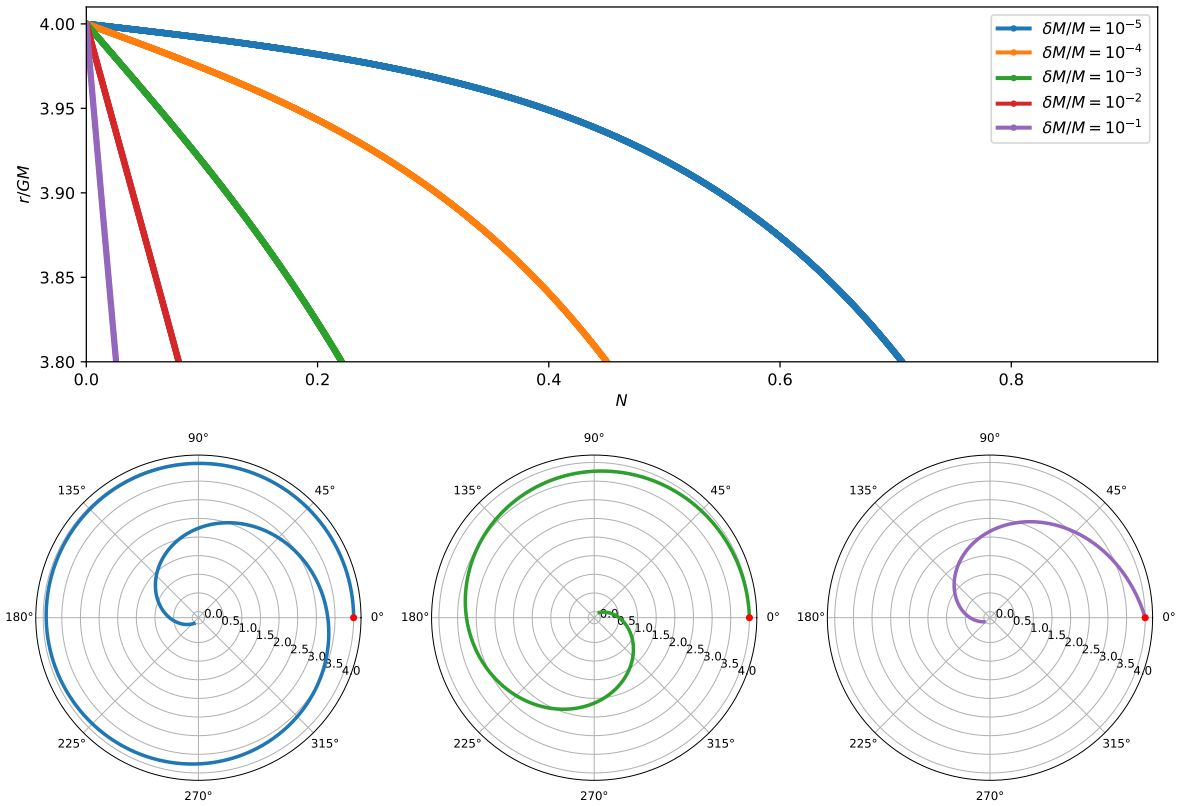



FIG. 15. Radial coordinate $\tilde{r} = r/G\,M$ of trajectories subject to perturbations $\delta M$ starting from the unstable circular orbit for $\tilde{L} = L/G\,M = 4$ (top panel); trajectories subject to the perturbation $\delta M/M = 10^{-5}$ (bottom left panel), $\delta M/M = 10^{-3}$ (bottom center panel) and $\delta M/M = 10^{-1}$ (bottom right panel).


### Acknowledgments

This work has been carried out in the framework of the activities of the National Group for Mathematical Physics (GNFM/INdAM). R.C. and A.G. are partially supported by the INFN grant FLAG.


### Appendix A: Equivalent analytic solutions

Introducing the change of variable $\tilde{x} = (3\,\rho\,x - 1)/12$, Eq. (15) can be written as [39, 40]

$$\left(\frac{\mathrm{d}\tilde{x}}{\mathrm{d}\varphi}\right)^2 = 4\,\tilde{x}^3 - g_2\,\tilde{x} - g_3 \ , \tag{A1}$$

with

$$g_2 = \frac{1}{12} - \frac{\rho^2}{4\,\alpha^2} \ , \qquad g_3 = \frac{1}{216} + \left(\frac{1}{24\,\alpha^2} - \frac{1}{16\,\beta^2}\right)\rho^2 \ , \tag{A2}$$

whose general solution is given by the Weierstrass elliptic function $\wp\,(z; g_2, g_3)$ of parameters $(g_2, g_3)$. Hence, the general solution of Eq. (15) can be expressed as

$$x(\varphi) = \frac{1}{\rho}\left[4\,\wp\left(\varphi + \tilde{\delta};\, g_2, g_3\right) + \frac{1}{3}\right] \ , \tag{A3}$$

where the constant $\tilde{\delta}$ is again obtained from the initial condition $x(\varphi_0) = x_0$.

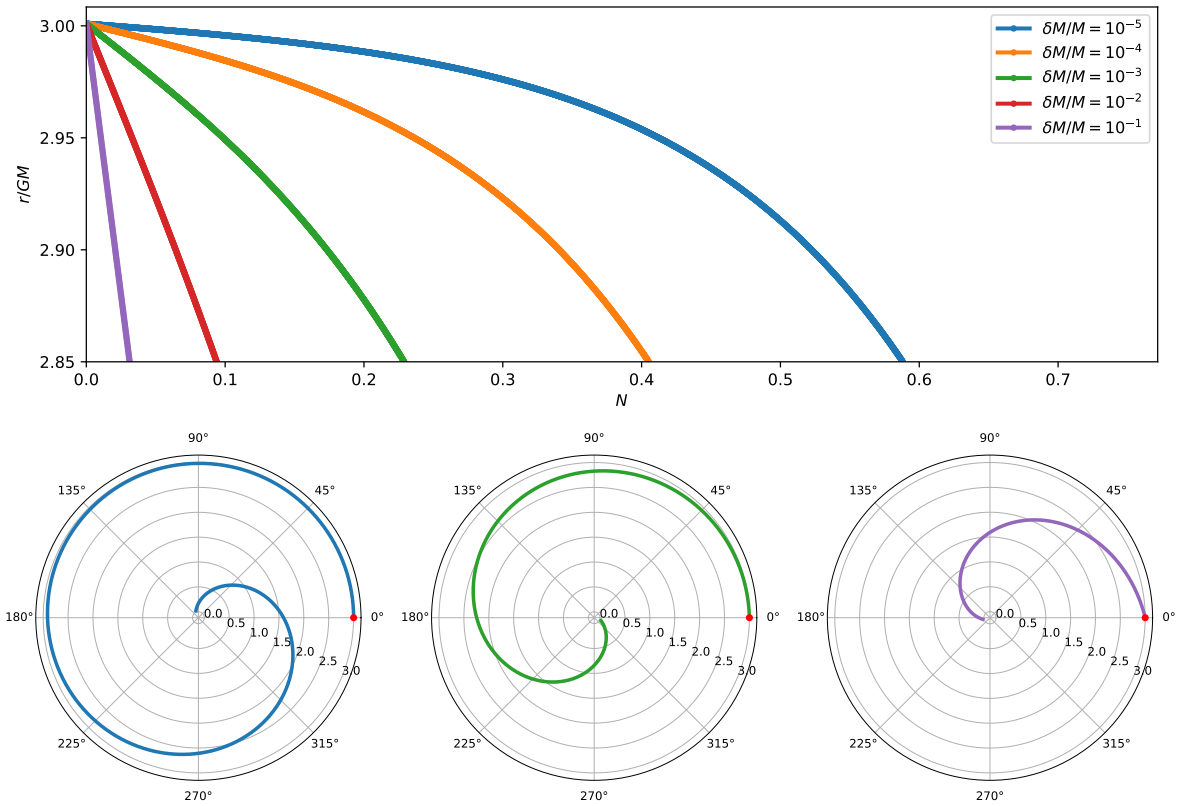



FIG. 16. Radial coordinate $\tilde{r} = r/G\,M$ of trajectories subject to perturbations $\delta M$ starting from the unstable circular orbit for $\tilde{L} = L/G\,M = 100$ (top panel); trajectories subject to the perturbation $\delta M/M = 10^{-5}$ (bottom left panel), $\delta M/M = 10^{-3}$ (bottom center panel) and $\delta M/M = 10^{-1}$ (bottom right panel).

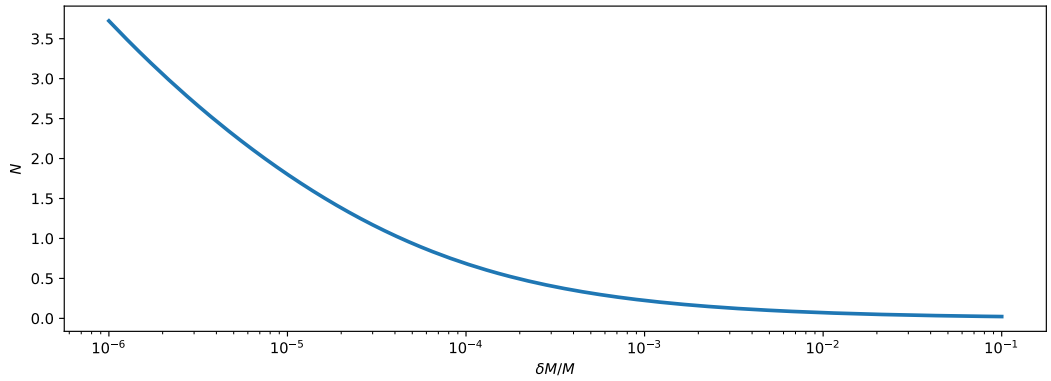



FIG. 17. Number of revolutions $N$ corresponding to a change of 5% in the radial coordinate as a function of the perturbation $\delta M/M$ ranging from $10^{-6}$ to $10^{-1}$.

Moreover, the Weierstrass elliptic function $\wp$ can be written in terms of Jacobi's elliptic function sn as

$$\wp(z) = e_1 + \frac{e_3 - e_1}{\mathrm{sn}^2\left(z\sqrt{e_3 - e_1},\, \bar{k}\right)} \,, \qquad \text{with } \bar{k} = \sqrt{\frac{e_2 - e_1}{e_3 - e_1}} \,, \tag{A4}$$

where $e_1$, $e_2$, $e_3$ are the roots of the polynomial on the right-hand side of Eq. (A1), i.e.

$$4\,\tilde{x}^3 - g_2\,\tilde{x} - g_3 = 4\,(\tilde{x} - e_1)\,(\tilde{x} - e_2)\,(\tilde{x} - e_3) \,, \tag{A5}$$

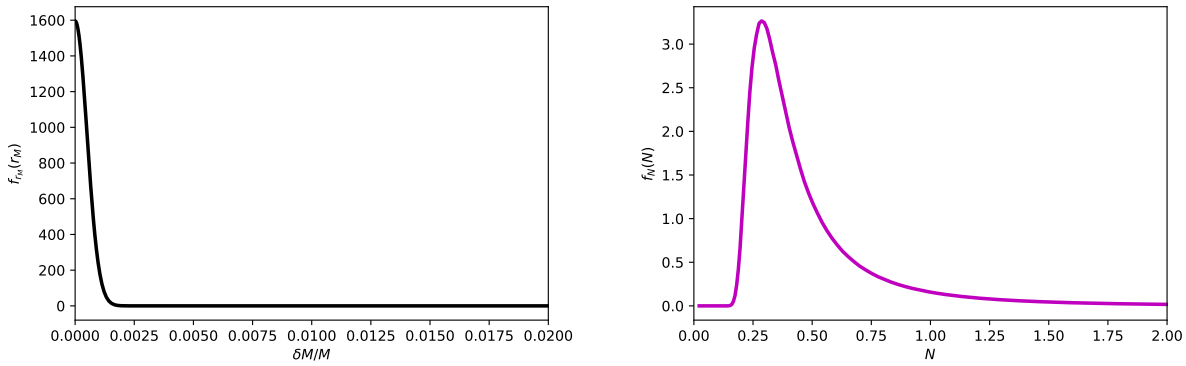



FIG. 18. Probability density function of the perturbation $\delta M \sim \mathcal{N}^* \left(\mu_{\delta M} = 0, \sigma^2_{\delta M} = 0.0005^2\right)$ (left panel) and corresponding probability density function of the number of revolutions $N$ after which the variation of the radial position of the particle amounts to 5% of the initial value (right panel).

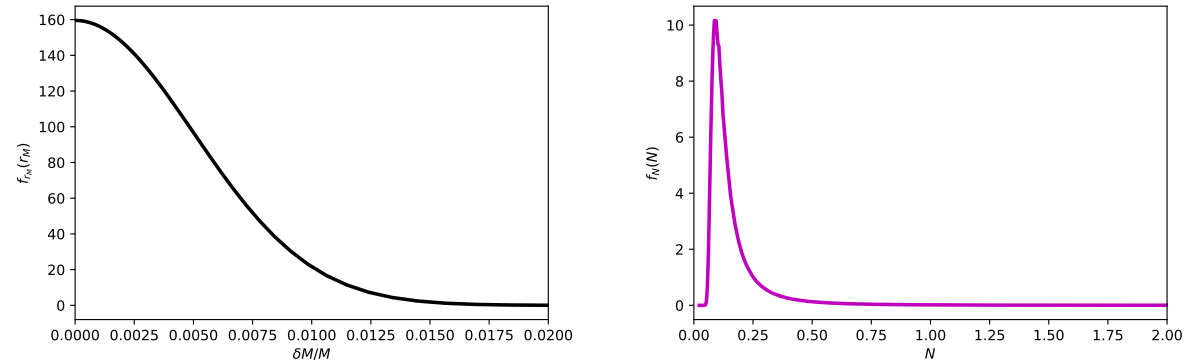



FIG. 19. Probability density function of the perturbation $\delta M \sim \mathcal{N}^* \left(\mu_{\delta M} = 0, \sigma^2_{\delta M} = 0.005^2\right)$ (left panel) and corresponding probability density function of the number of revolutions $N$ after which the variation of the radial position of the particle amounts to 5% of the initial value (right panel).

with $e_1 + e_2 + e_3 = 0$. Taking into account that, for $j = 1, 2, 3$,

$$e_j = \frac{\rho}{4} x_j - \frac{1}{12} \ , \tag{A6}$$

we see that $\bar{k} = k$ in Eq. (23). Making use of the relation [39]

$$\wp(z) = e_1 + \frac{e_3 - e_1}{\mathrm{sn}^2\left(z\sqrt{e_3 - e_1},\, k\right)} = e_1 + \frac{e_2 - e_1}{k^2\,\mathrm{sn}^2\left(z\sqrt{e_3 - e_1},\, k\right)} \ , \tag{A7}$$

the solution (A1) can be also written as

$$x(\varphi) = x_1 + \frac{x_2 - x_1}{k^2\,\mathrm{sn}^2\left(\frac{\varphi}{2}\sqrt{\rho\,(x_3 - x_1)} + \bar{\delta},\, k\right)} \ , \tag{A8}$$

where $\bar{\delta} = \tilde{\delta}\sqrt{\rho\,(x_3 - x_1)}/2$. Finally, making use of the relation [39]

$$\wp(z) = e_1 + (e_2 - e_1)\,\mathrm{sn}^2\left(\left(z - \omega_3\right)\sqrt{e_1 - e_3},\, k\right) \ , \tag{A9}$$

where $\wp\left(\omega_3/2\right) = e_3$, Eq. (A1) can be finally written as

$$x(\varphi) = x_1 + (x_2 - x_1)\,\mathrm{sn}^2\left(\frac{\varphi}{2}\sqrt{\rho\,(x_3 - x_1)} + \delta^*,\, k\right) \ , \tag{A10}$$

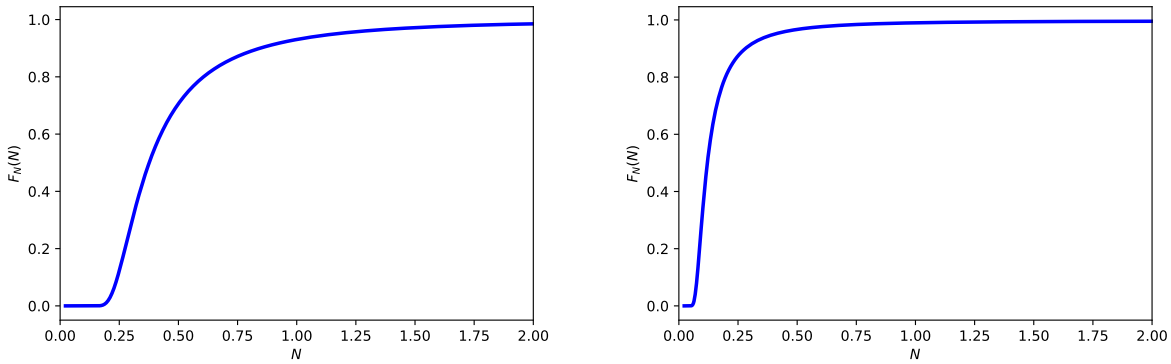



FIG. 20. Cumulative distribution functions of the random variable $N$ resulting from a probability density function of the perturbation $\delta M \sim \mathcal{N}^*\left(\mu_{\delta M} = 0, \sigma^2_{\delta M} = 0.0005^2\right)$ (left panel) and $\mathcal{N}^*\left(\mu_{\delta M} = 0, \sigma^2_{\delta M} = 0.005^2\right)$ (right panel).

where $\delta^* = (\tilde{\delta} - \omega_3)\sqrt{\rho\,(x_3 - x_1)}/2$. Of course, the three expressions (22), (A8) and (A10) are perfectly equivalent.


[1] S. M. Carroll, *Spacetime and geometry: An introduction to general relativity*, San Francisco, USA: Addison-Wesley, 1 ed., 2004.
[2] R. M. Wald, *General Relativity*, Chicago University Press, Chicago, USA, 1984.
[3] B. P. Abbott *et al.* [LIGO Scientific and Virgo Collaborations], Phys. Rev. Lett. **116**, no. 6, 061102 (2016) [arXiv:1602.03837 [gr-qc]].
[4] R. P. Geroch and J. H. Traschen, Phys. Rev. D **36**, 1017 (1987).
[5] S. W. Hawking, Commun. Math. Phys. **43**, 199 (1975) Erratum: [Commun. Math. Phys. **46**, 206 (1976)].
[6] S. W. Hawking, Phys. Rev. D **14**, 2460 (1976).
[7] D. N. Page, Phys. Rev. Lett. **71**, 3743 (1993) [hep-th/9306083].
[8] S. W. Hawking, Phys. Rev. D **72**, 084013 (2005) [hep-th/0507171].
[9] S. Hollands and R. M. Wald, Phys. Rept. **574**, 1 (2015) [arXiv:1401.2026 [gr-qc]].
[10] O. C. Stoica, Adv. High Energy Phys. **2018**, 4130417 (2018) [arXiv:1807.05864 [gr-qc]].
[11] A. Giusti, Int. J. Geom. Meth. Mod. Phys. **16**, no. 03, 1930001 (2019) [Preprint: researchgate.net/publication/330250722].
[12] R. Casadio and A. Orlandi, JHEP **1308**, 025 (2013) [arXiv:1302.7138 [hep-th]].
[13] R. Casadio, A. Giugno, O. Micu and A. Orlandi, Phys. Rev. D **90**, no. 8, 084040 (2014) [arXiv:1405.4192 [hep-th]].
[14] R. Casadio, A. Giugno and A. Orlandi, Phys. Rev. D **91**, no. 12, 124069 (2015) [arXiv:1504.05356 [gr-qc]].
[15] S. Capozziello, M. De laurentis and A. Stabile, Class. Quant. Grav. **27**, 165008 (2010) [arXiv:0912.5286 [gr-qc]].
[16] T. P. Sotiriou and V. Faraoni, Phys. Rev. Lett. **108**, 081103 (2012) [arXiv:1109.6324 [gr-qc]].
[17] T. P. Sotiriou and S. Y. Zhou, Phys. Rev. Lett. **112**, 251102 (2014) [arXiv:1312.3622 [gr-qc]].
[18] P. O. Mazur and E. Mottola, gr-qc/0109035.
[19] C. B. M. H. Chirenti and L. Rezzolla, Class. Quant. Grav. **24**, 4191 (2007) [arXiv:0706.1513 [gr-qc]].
[20] P. Nicolini, A. Smailagic and E. Spallucci, Phys. Lett. B **632**, 547 (2006) [gr-qc/0510112].
[21] A. Bonanno and M. Reuter, Phys. Rev. D **62**, 043008 (2000) [hep-th/0002196].
[22] G. Raposo, P. Pani, M. Bezares, C. Palenzuela and V. Cardoso, Phys. Rev. D **99**, no. 10, 104072 (2019) [arXiv:1811.07917 [gr-qc]].
[23] R. Casadio, arXiv:1305.3195 [gr-qc].
[24] R. Casadio, A. Giugno and O. Micu, Int. J. Mod. Phys. D **25**, no. 02, 1630006 (2016) doi:10.1142/S0218271816300068 [arXiv:1512.04071 [hep-th]].
[25] R. Casadio, A. Giugno and A. Giusti, Gen. Rel. Grav. **49**, no. 2, 32 (2017) [arXiv:1605.06617 [gr-qc]].
[26] R. Casadio, A. Giugno, A. Giusti and O. Micu, Eur. Phys. J. C **77**, no. 5, 322 (2017) [arXiv:1701.05778 [gr-qc]].
[27] B. L. Hu and E. Verdaguer, Living Rev. Rel. **11**, 3 (2008) [arXiv:0802.0658 [gr-qc]].
[28] K. Schwarzschild, Sitzungsber. Preuss. Akad. Wiss. Berlin (Math. Phys. ) **1916**, 189 (1916) [physics/9905030].
[29] K. Schwarzschild, Sitzungsber. Preuss. Akad. Wiss. Berlin (Math. Phys. ) **1916**, 424 (1916) [physics/9912033 [physics.hist-ph]].
[30] A. Papoulis and S. U. Pillai, *Probability, Random Variables, and Stochastic Processes*, New York, USA: McGraw-Hill, 4 ed., 2002.
[31] H. Falcke, J. Phys. Conf. Ser. **942**, no. 1, 012001 (2017) [arXiv:1801.03298 [astro-ph.HE]].
[32] A. Ricarte and J. Dexter, Mon. Not. Roy. Astron. Soc. **446**, 1973 (2015) [arXiv:1410.2899 [astro-ph.HE]].

[33] C. Goddi *et al.*, Int. J. Mod. Phys. D **26**, no. 02, 1730001 (2017) [arXiv:1606.08879 [astro-ph.HE]].
[34] V. Dokuchaev, Int. J. Mod. Phys. D **28**, 1941005 (2019) [arXiv:1812.06787 [astro-ph.HE]].
[35] B. J. Carr, J. Mureika and P. Nicolini, JHEP **1507**, 052 (2015) [arXiv:1504.07637 [gr-qc]].
[36] J. R. Mureika, Phys. Lett. B **789**, 88 (2019) [arXiv:1812.01999 [gr-qc]].
[37] C. Rovelli and F. Vidotto, Int. J. Mod. Phys. D **23**, no. 12, 1442026 (2014) [arXiv:1401.6562 [gr-qc]].
[38] T. De Lorenzo, A. Giusti and S. Speziale, Gen. Rel. Grav. **48**, no. 3, 31 (2016) Erratum: [Gen. Rel. Grav. **48**, no. 8, 111 (2016)] [arXiv:1510.08828 [gr-qc]].
[39] E. T. Whittaker and G. N. Watson, *A course of modern analysis*, Cambridge University Press, 4 ed., 1927.
[40] G. Pastras, "Four Lectures on Weierstrass Elliptic Function and Applications in Classical and Quantum Mechanics," arXiv:1706.07371 [math-ph].